streams. Thus, the data clearly indicate the effects of pyrolysis-gas injection, i.e., blockage and consumption of boundary-layer oxygen in gas-phase chemical reactions.

Included in the lower part of Fig. 3 are the theoretical correlations for the char-removal parameter in air for a low-density phenolic-nylon composite as presented in Wakefield et al.[5] Theoretical relations were obtained assuming 1) an analytical model with diffusion blockage, but without gas-phase chemical reactions; and 2) a model which included the influence of chemical reactions between the pyrolysis gases and the stream species in addition to the blockage effect. To perform these calculations for a particular case, the elemental compositions of the stream, pyrolysis gases, and surface char were specified to match the experimental program of Ref. 5. The data from the present program, which exhibit the expected variation with $\dot{m}_{vp}/\Delta\dot{m}_{cr}$, fall beween the char-removal rates predicted using the two theoretical correlation models. The lack of better quantitative agreement with the theory for a reactive pyrolysis gas is attributed to differences in materials and in the flow conditions of the present tests and those of Ref. 5.

### *Comparative performance in the three environments*

The external degradation parameter, i.e., surface recession, indicates that air is the most severe environment, followed closely by $N_2/CO_2$, with inert $N_2$ the least severe. The rate of internal degradation of a phenolic-nylon material depends only upon the in-depth temperature profile. As discussed by Parker and Winkler,[11] the degradation process itself is anaerobic and independent of the mode of heating. Further, except possibly at very high stagnation pressures and low heating rates, the pyrolysis gas flow prevents the boundary-layer gases from penetrating the surface due to the very high pressures generated in the decomposition zone. However, the composition of the external environment is an important factor in the internal degradation process, since the chemical reactions at the surface and in the boundary layer determine the thickness of char layer and, to some degree, the surface temperature. Since the temperature at the char/pyrolysis interface depends on the degradation properties of the material and is usually assumed to be a constant, the thermal gradient (and, hence, the rate at which energy is supplied to the pyrolysis zone) across the char is dependent upon the composition of the external environment.

If one considers the data from those tests with comparable flow conditions, one finds an effect of gas composition. For tests with different gas compositions to be considered as comparable flow conditions, it was necessary that $H_{Cl}$ and $P_s$ be approximately equal. Using these criteria, conditions 1 and 8, 3 and 10, 12 and 18, and 7, 14, and 20 provide material performance data at comparable conditions.

The internal interface velocities in air were generally about 30% higher than those in $N_2$ and about 15% higher than those in $N_2/CO_2$, even though the surface temperatures in air were only slightly higher (100–170°F) than in $N_2$. The surface temperatures in the $N_2/CO_2$ mixture were similar to those observed in the other two streams. Further analysis of the data indicates that the differences between the internal degradation rates measured in air and those measured in nitrogen streams become more pronounced with increasing stagnation pressure. This dependence on pressure is believed to reflect the effects of surface combustion. First, the exothermic surface combustion increases heating to the surface and, since the increased char removal results in a thinner char cap, the thermal gradient across the char cap is larger. Both factors contribute to a higher rate of conduction of energy across the char layer to supply the degradation process.

### References


[1] Vojvodich, N. S. and Pope, R. B., "Effect of Gas Composition on the Ablation Behavior of a Charring Material," *AIAA Journal*, Vol. 2, No. 3, March 1964, pp. 536–542.

[2] Lundell, J. H., Wakefield, R. M., and Jones, J. W., "Experimental Investigation of a Charring Ablative Material Exposed to Combined Convective and Radiative Heating," *AIAA Journal*, Vol. 3, No. 11, Nov. 1965, pp. 2087–2095.

[3] Clark, R. K., "Effect of Environmental Parameters on the Performance of Low-Density Silicone-Resin and Phenolic-Nylon Ablation Materials," TND-2543, Jan. 1965, NASA.

[4] Lundell, J. H., Dickey, R. R., and Jones, J. W., "Performance of Charring Ablative Materials In The Diffusion-Controlled Surface Combustion Regime," *AIAA Journal*, Vol. 6, No. 6, June 1968, pp. 1118–1126.

[5] Wakefield, R. M., Lundell, J. H., and Dickey, R. R., "Effects of Pyrolysis-Gas Chemical Reactions on Surface Recession of Charring Ablators," *Journal of Spacecraft and Rockets*, Vol. 6, No. 2, Feb. 1969, pp. 122–128.

[6] McLain, A. G., Sutton, K., and Walberg, G. D., "Experimental and Theoretical Investigation of the Ablative Performance of Five Phenolic-Nylon-Based Materials," TN D-4374, April 1968, NASA.

[7] Bertin, J. J., Conine, W. D., and Nipper, M. J., "Surface Recession of Phenolic Nylon in Low-Density Arc-Heated Air," *AIAA Journal*, Vol. 7, No. 11, Nov. 1969, pp. 2163–2165.

[8] Scala, S. M. and Gilbert, L. M., "Sublimation of Graphite at Hypersonic Speeds," *AIAA Journal*, Vol. 3, No. 9, Sept. 1965, pp. 1635–1644.

[9] Kratsch, K. M., Hearne, L. F., and McChesney, H. R., "Theory for the Thermophysical Performance of Charring Organic Heat-Shield Composites," Rept. 803099, Oct. 1963, Lockheed Missiles and Space Co., Sunnyvale, Calif.

[10] Baily, H. E., *Equilibrium Thermodynamic Properties of Three Engineering Models of the Martian Atmosphere*, SP-3021, NASA, 1965.

[11] Parker, J. A. and Winkler, E. L., "The Effects of Molecular Structure on the Thermophysical Properties of Phenolics and Related Polymers," TR R-276, Nov. 1967, NASA.


# Thermal Curvature Time Constants of Thin-Walled Tubular Spacecraft Booms


F. R. VIGNERON*

*Communications Research Center, Department of Communications, Ottawa, Canada*


SEVERAL "time constants" associated with thin-walled tubular spacecraft booms have arisen in astrodynamics applications: one for average temperature rise after the boom emerges from shadow into sun, another associated with thermal flutter, another associated with the establishment of thermal curvature resulting from a solar step function input, and, as will be seen, yet another associated with thermal curvature resulting from a periodically varying input such as is experienced by a boom rotating end over end in the ecliptic plane. These constants are interrelated, but they all have different quantitative values; this Note addresses the latter two, which are important to the development of theories of solar-induced despin of the Alouette and ISIS satellites.[1,2] In developing a solar despin theory, Etkin and Hughes hypothesized that solar induced curvature would be governed by a first-order linear equation of the form,

$$[\partial\kappa_T(x,t)/\partial t] + (1/T)\kappa(x,t) = f(x,t) \qquad (1)$$

where $\kappa_T(x,t)$ is the thermally induced curvature, $x$ is the length coordinate of the boom, $t$ is time, $f(x,t)$ is an external radiation input, and $T$ is a thermal time constant. No particular restrictions were placed on the range of application of the

Received June 10, 1970; revision received July 30, 1970.

* Research Scientist, National Space Telecommunications Laboratory.

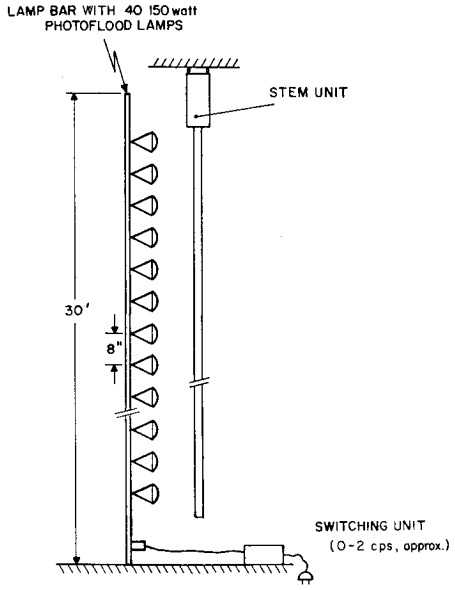


**Fig. 1 Configuration for experimental measurements.**

equation, as virtually no appropriate recorded experimental data were available. In the following, experimental evidence and related analyses are presented which show that the simple Eq. (1) applies when $f(x,t)$ is periodic with sufficiently short period, and that a distinction must be made between periodic and step-function inputs.

### Experimental Measurements on Thermally Induced Curvature

Gerrish[3] measured response to a solar step-function input by a 0.5-in.-diam beryllium copper STEM† boom using photoflood lamps arranged as shown in Fig. 1. Deflection response to the step function was found to approximate an exponential rise curve. Values of the appropriate time constant were found to be between 2.16 and 3.16 sec, depending on orientation of the boom's seam relative to the heat source. The time constant was largest when the seam faced the source. As a result of the measurements, Etkin and Hughes adopted a value of $T = 2.7$ sec for use in Eq. (1), a value which has been used to date. A value of $T = 17$ sec was similarly established for 1-in.-diam steel STEMs.

This writer subsequently measured response to a periodically varying input by a 0.5-in.-diam STEM, using the same configuration as shown in Fig. 1.[4] The lamp input and boom deflection were monitored by photocell devices and a recording oscilloscope. An observed phase lag angle $\phi_0$ between lamp input and resulting deflection, measured over a frequency range embracing the first vibrational resonance is shown in Fig. 2. A time constant equal to 1.55 sec was deduced from the data at frequencies less than 0.20 cps. The value so obtained was attributable almost entirely to thermal lag effects (rather than frictional effects). Measurements of response to a step input were repeated and were found to confirm Gerrish's original measurements.

### Analysis of a Boom Subjected to a Periodic Input

Let us assume that the boom is a closed, thin-walled tube. The temperature distribution in the material satisfies the conduction equation,

$$\partial T/\partial t = D\nabla^2 T \tag{2}$$

where $T$ is temperature, $D$ is the thermal diffusivity, and $\nabla^2$ is the Laplacian. The heat rate per unit area at the outer

† STEM—Stored Tubular Extendable Member, manufactured by SPAR Aerospace, Ltd., Malton, Ontario, Canada.

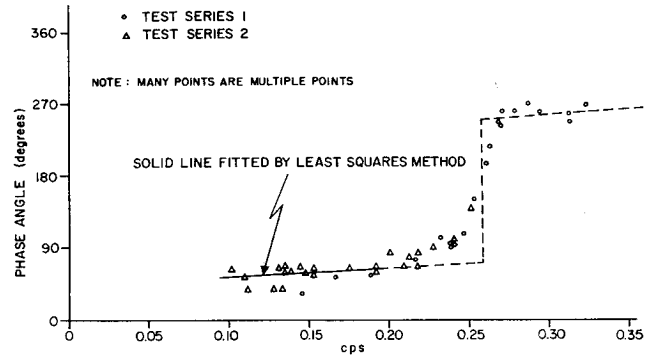


**Fig. 2 Measured data.**

boundary as a result of direct lamp radiation is, approximately,

$$q_s = \alpha Q(t)\cos^+\psi \tag{3}$$

where $Q(t)$ is the heat rate from the lamps, $\alpha$ is the absorptivity, $\psi$ is measured with respect to the lamps as is shown in Fig. 3 and $\cos^+\psi$ is defined as $\cos\psi$ when $-\pi/2 < \psi < \pi/2$ and zero when $\pi/2 < \psi < 3\pi/2$. The function $Q(t)$ generated by the lamp switching unit was found by photocell measurement to be a periodic square wave, which could be approximated by a truncated Fourier series expansion as

$$Q(t) = S[\tfrac{1}{2} - (2/\pi)\cos\omega t] \tag{4}$$

where $S$ is the lamp intensity and $\omega$ is the switching frequency.

The re-emitted heat rate per unit area on both inner and outer boundaries is $e\sigma T^4$, where $e$ is emissivity and $\sigma$ is Boltzmann's constant, $0.1713 \times 10^{-8}$ Btu/ft²-hr-(°R)⁴. The rate of heat reabsorption per unit area at the inner boundary as a result of internal radiation exchange may be conveniently taken to be approximately $e\sigma\bar{T}^4$, where $\bar{T}$ is the average temperature of the internal wall.[5,6] Conduction along the length may be neglected, as the tubes are very long and have small cross-sectional area. The ratio of wall thickness $d$ to tube radius $R$ is small, and therefore, radial conduction may be approximated by the sum of the radial heat flows at the boundaries. Utilizing these approximations, the Laplacian, in cylindrical coordinates $(R,\psi,z)$ becomes

$$\nabla^2 T = (1/R^2)(\partial^2 T/\partial\psi^2) - (2e\sigma T^4/kd) + (e\sigma\bar{T}^4/kd) + [\alpha Q(t)/kd]\cos^+\psi \tag{5}$$

and consequently Eq. (2) becomes

$$(\partial T/\partial t) - (k/R^2\rho c)(\partial^2 T/\partial\psi^2) + (2e\sigma/\rho dc)T^4 - (e\sigma/\rho dc)\bar{T}^4 = (\alpha/\rho dc)Q(t)\cos^+\psi \tag{6}$$

In the previous equations, $k$ is the thermal conductivity, $\rho$ is the mass per unit length, and $c$ is the specific heat of the ma-

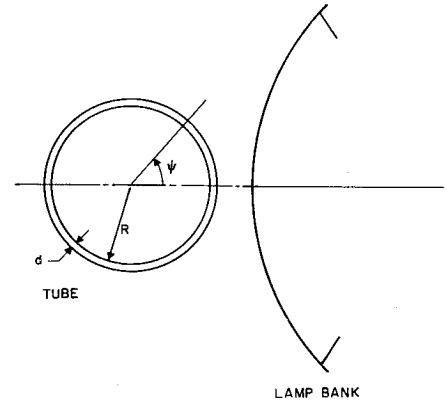


**Fig. 3 Tube section relative to lamp bank.**

terial. Equation (6) is identical to Eq. (15) of Ref. 5. Solutions of the equation for static cases, obtained by numerical computation, show good agreement with experimental results for STEMs of the type used on Alouette satellites.

The heat rate $\mathbf{q}$ is given by

$$\mathbf{q} = -k\nabla T \tag{7}$$

Integration of Eq. (2) over the tube volume, application of the divergence theorem to the right-hand side, and utilization of Eq. (7) results in

$$\frac{\partial}{\partial t}\iiint_V T dv = -\frac{1}{\rho c}\iint_A \mathbf{q}\cdot d\mathbf{a} \tag{8}$$

where $d\mathbf{a}$ is a directed surface element, $A$ denotes surface area, $dv$ is a volume element, and $V$ denotes volume of the tube. The average temperature is, by definition

$$\iiint_V T dv/V$$

The surface integral of the heat rate equals the net heat flow at the tube boundaries, as specified previously. Thus, Eq. (8) becomes

$$2\pi R d\frac{d\bar{T}}{dt} - \frac{e\sigma}{\rho c}\int_0^{2\pi}\bar{T}^4 d\psi + \frac{2e\sigma}{\rho c}\int_0^{2\pi} T^4 d\psi = \frac{\alpha R}{\rho c}Q(t)\int_{-\pi/2}^{\pi/2}\cos\psi d\psi \tag{9}$$

The temperature may be expressed as $T = \bar{T}(1 + \Delta\theta)$, where $\Delta\theta$ is a dimensionless function of $\psi$. It follows from the definition of $\bar{T}$ that $\int\Delta\theta dv = 0$. From measurements and previous work, it is known that $\Delta\theta \ll 1$; consequently $T^4 \doteq \bar{T}^4(1 + 4\Delta\theta)$, and then $\int T^4 dv \doteq \int\bar{T}^4 dv$. The previous equation then becomes

$$(d\bar{T}/dt) + (e\sigma/\rho dc)\bar{T}^4 = (\alpha/\pi\rho dc)Q(t) \tag{10}$$

It is convenient to normalize temperatures with respect to $T_{st}$, the average temperature of full intensity steady-state conditions, which can be deduced to be

$$T_{st} = (\alpha S/\pi e\sigma)^{1/4} \tag{11}$$

With $\theta = T/T_{st}$ and $\phi = \omega t$, Eq. (6) takes the form

$$(\partial\theta/\partial\phi) - (m\partial^2\theta/\partial\psi^2) + 2h\theta^4 - h\bar{\theta}^4 = \pi h\cos^+\psi[\tfrac{1}{2} - (2/\pi)\cos\phi] \tag{12}$$

where $m = k/\rho cR^2\omega$ and $h = T_{st}^3 e\sigma/\rho dc\omega$. Similarly, Eq. (10) becomes

$$(\partial\bar{\theta}/\partial\phi) + h\bar{\theta}^4 = h[\tfrac{1}{2} - (2/\pi)\cos\phi] \tag{13}$$

where $\bar{\theta}$ equals $\bar{T}/T_{st}$.

To determine average temperature behavior let us assume a solution of Eq. (13) in the form,

$$\bar{\theta} = \bar{\theta}_0[1 + \epsilon(\phi)] \tag{14}$$

where $\bar{\theta}_0$ is a constant and $\epsilon(\phi)$ is a time-varying perturbation. Substitution into Eq. (13) results in, approximately,

$$(d\epsilon/d\phi) + 4h\bar{\theta}_0^3\epsilon = h[(1/2\bar{\theta}_0) - \bar{\theta}_0^3] - (2h/\pi\bar{\theta}_0)\cos\phi \tag{15}$$

provided that $\epsilon(\phi) \ll 1$. A steady-state periodic solution of Eq. (15) is obtained by choosing $\bar{\theta}_0 = (\tfrac{1}{2})^{1/4}$ (in which case the secular term of the right-hand-side of the equation vanishes identically for all $\phi$), and then solving for $\epsilon(\phi)$. After doing this, resubstitution into Eq. (14) yields,

$$\bar{\theta} = \bar{\theta}_0\{1 - 2h\cos(\phi - \phi_0)/\pi\bar{\theta}_0[1 + (4h\bar{\theta}_0^3)^2]^{1/2}\} \tag{16}$$

Physical parameters of beryllium copper STEMs used in the experiments described in Sec. 2 are listed in the first column of Table 1. For the range of frequencies of the experiments $h < 0.001$. Evaluation of Eq. (16) with these values leads one to the conclusion that $\bar{\theta} = \bar{\theta}_0[1 \pm 0.0008] \doteq (\tfrac{1}{2})^{1/4}$ for this type of test.

**Table 1 Stem properties**

| | $\frac{1}{2}$-in. BeCu | 1-in. steel |
|---|---|---|
| Tape width, ft | 0.166 | 0.333 |
| Thickness $d$, ft | 0.000167 | 0.000416 |
| Mass/length, slug/ft | 0.000449 | 0.00212 |
| Material density, lb/ft$^3$ | 500 | 490 |
| Absorptivity $\alpha$ (solar source)[a] | 0.45 | 0.48 |
| Emissivity $e$ | 0.1 | 0.24 |
| Specific heat $c$, Btu/lb-°R | 0.1 | 0.12 |
| Thermal expansion coefficient $\alpha_T$, 1/°R | $10.5 \times 10^{-6}$ | $6.5 \times 10^{-6}$ |
| Thermal conductivity $k$, Btu/hr-ft-°R | 60[b] | 30[c] |

[a] It is assumed that the photoflood lamp source adequately simulates a solar source.
[b] Values range from 44–70, depending on the condition of the material; for precipitation-hardened BeCu, $k = 60$.
[c] ASM Metals Handbook, 1948.

An expression for thermal curvature may be deduced from Ref. 7 to be

$$\kappa_T = \kappa_{TO}\int_0^{2\pi}\theta\cos\psi d\psi \tag{17}$$

where $\kappa_{TO} = \alpha_T T_{st}/\pi R$ and $\alpha_T$ is the coefficient of thermal expansion. Let us multiply Eq. (12) by $\kappa_{TO}\cos\psi$ and integrate it over $\psi$ from 0 to $2\pi$. With the aid of Eq. (17), the first term becomes $\partial\kappa_T/\partial\phi$. Integration of the second term by parts twice, and specification of continuity of $\theta$ and $\partial\theta/\partial\psi$ results in transformation of the term to $m\kappa_T$. In the third term, upon letting $\theta = \bar{\theta}(1 + \Delta\theta)$, and $\theta^4 = \bar{\theta}^4(1 + 4\Delta\theta)$, one may transform to $8h\bar{\theta}^3\kappa_T$. The fourth term disappears. The right-hand side may be integrated to give

$$(\partial\kappa_T/\partial\phi) + (m + 8h\bar{\theta}^3)\kappa_T = (\pi^2/2)\kappa_{TO} \times h[\tfrac{1}{2} - (2/\pi)\cos\phi] \tag{18}$$

Hence the thermal curvature variation is described by a first-order equation, exactly of the form assumed by Etkin and Hughes.[1,2] When $\bar{\theta}^3$ is approximately constant (as it is for a periodically varying input) the behavior is characterized by a time constant $(m + 8h\bar{\theta}_0^3)^{-1}$ which, in dimensional terms, is

$$T = \rho/[(k/cR^2) + (8\tfrac{1}{2}^{3/4}T_{st}^3 e\sigma/d)] \tag{19}$$

The two terms in the denominator of Eq. (19) signify that the time constant is influenced by two factors, heat conduction around the circumference of the tube, and radiation heat transfer, which is as expected.

### Results and Discussion

With STEM parameters listed in Table 1 and a (measured) average tube radius of 0.265 in., Eq. (19) yields $T = 1.45$ sec. The value agrees to within 7% with the measured value of 1.55 sec. The deduction of $T$ from Eq. (18) requires that $\bar{\theta}$ be approximately constant, which it is when the heat input is periodic with a sufficiently fast period (e.g., the test conditions used herein). Note that when the input is a step function, $\bar{\theta}$ will vary with time, the appropriate equation corresponding to Eq. (18) will be nonlinear, and consequently a different time constant may be expected. This behavior appears to be confirmed by Gerrish's experiments.

Equations similar in form to Eqs. (12), (16), and (18) may be obtained for the case when the STEMs are rotating end over end in the ecliptic plane, as is the case for the Alouette and ISIS spacecraft.[8] The average temperature $\bar{\theta}_0$ for this case is found to be $(2/\pi)^{1/4}$, resulting in a time constant,

$$T = \rho/(k/cR^2) + [8(2/\pi)^{3/4}T_{st}^3 e\sigma/d] \tag{20}$$

The value of $T$ for Alouette I, which employs 1-in.-diam steel STEMs with properties listed in Table 1, is 11.5 sec. For Alouette II and ISIS-I, employing beryllium copper 0.5-in.-diam STEMs, $T$ of Eq. (20) is 1.3 sec.

### Concluding Remarks

The experimental and analytical evidence strongly indicate that the appropriate time constant for despin theories is as given by Eq. (20). Allowing for variation in radius (it appears that the radius of STEMs slightly increases over a period of years) and other parameters, it appears that the upper bound values of $T$ for satellite applications are about 1.6 and 14 sec for beryllium copper and steel STEMs, respectively.

### References

[1] Etkin, B. and Hughes, P. C., "Spin Decay of a Class of Satellites Caused by Solar Radiation," Rept. 107, July 1965, Univ. of Toronto, Institute for Aerospace Studies (UTIAS).

[2] Etkin, B. and Hughes, P. C., "Explanation of the Anomalous Spin Behaviour of Satellites with Long Flexible Antennas," *Journal of Spacecraft*, Vol. 4, No. 9, Sept. 1967, pp. 1139–1145.

[3] Gerrish, R. J., "Thermal Bending Response Times for Alouette I and Alouette B Sounder Antennae," private communication, 1965, Ottawa, Canada.

[4] Vigneron, F. R., "Experiments on Lateral Vibrations of Alouette Sounder Antennas," DRTE Rept. 1170, Nov. 1966, Dept. of National Defence, Ottawa, Canada.

[5] Mar, J. and Garrett, T., "Mechanical Design and Dynamics of the Alouette Spacecraft," *Proceedings of IEEE*, Vol. 57, No. 6, June 1969, pp. 882–896.

[6] Paghis, I., Franklin, C. A., and Mar, J., "Alouette I, The First Three Years in Orbit," DRTE Rept. 1159, March 1967, Dept. of National Defence, Ottawa, Canada.

[7] Boley, B. A. and Weiner, J. H., *Theory of Thermal Stresses*, Wiley, New York, 1960, pp. 307–314.

[8] Vigneron, F. R., "Transient Temperature and Thermal Curvature Behavior of Sounder Antennas on Alouette Satellites," DRTE Rept. 1167, Nov. 1966, Dept. of National Defence, Ottawa, Canada.

# Prediction of Interstitial Gas Pressure in Multilayer Insulation during Rapid Evacuation

K. M. Kneisel* and F. O. Bennett†
*Convair Division of General Dynamics, San Diego, Calif.*

THE use of multiple-layer radiation shields for insulating cryogenic propellant tanks on long-term missions has long been considered. However, the fragile nature of the shields ($\frac{1}{4}$-mil aluminized Mylar) has necessitated a considerable development program for designing a light weight, structurally sound insulation system. One problem has been the prediction of the insulation stresses caused by the evacuation of the helium purge gas during ascent. These stresses can be estimated for a particular shape blanket using membrane theory if the pressure differential across the blanket can be determined.

The gas flow in most multilayer blankets is two-dimensional; however, a conservative estimate of the pressure differential can be made using the results of one-dimensional theory wherein the minimum linear flow path (distance from center of blanket to the nearest open edge) is used as the length dimension.

Presented as Paper 69-608 at the AIAA 4th Thermophysics Conference, San Francisco, Calif., June 16–18, 1969; submitted May 13, 1970; revision received July 1, 1970. This work was sponsored by NASA/MSFC on Contract NAS 8-18021 under the direction of E. H. Hyde.

* Senior Thermodynamics Engineer, Thermodynamics Group.
† Thermodynamics Engineer, Thermodynamics Group.

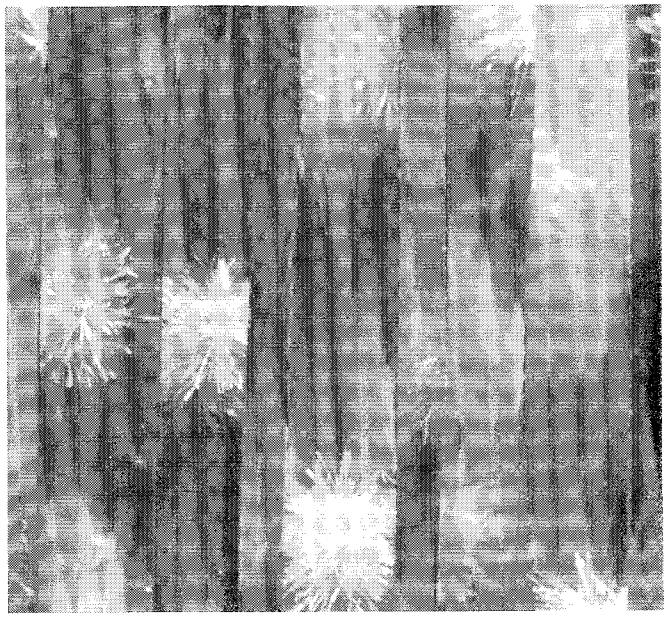

Fig. 1 Layers of Superfloc.

In multilayer insulation blankets, adjacent shields are spaced either by use of positive low-conductive spacers such as foam sheets, or by deforming each shield so that adjacent shields touch only over a minimal area. The effect of these spacers on the gas flow makes the flow problem too complex to solve analytically without empirical data. Therefore, we postulate a type of flow and force the solution of the analytical model to fit experimental data with the use of a correlation factor. This factor is a function o the layer density only for each particular type of insulation. The type of in ulation tested in this study was Superfloc (Fig. 1). In this insulation, the spacer consists of small tufts of Dacron needles.

### Analytical Model

We assume that the gas flow is analogous to continuum flow in a porous medium with constant permeability; it is one dimensional and isothermal; and the gas is perfect with constant fluid properties.

The mass flow rate is given by the equation $\dot{m} = (K/\mu) \times \rho(\partial P/\partial x)$ where $\mu$ is the mean gas viscosity evaluated at the average blanket temperature. $K$ is the insulation permeability and is a function of layer density only. It is to be determined experimentally for each type of insulation.

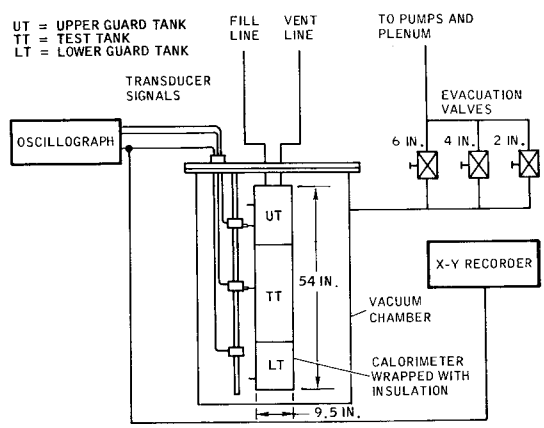


Fig. 2 Experimental apparatus schematic.